Biochimica et Biophysica Acta 1847 (2015) 286–293

Contents lists available at ScienceDirect

Biochimica et Biophysica Acta

journal homepage: www.elsevier.com/locate/bbabio

An irradiation density dependent energy relaxation in plant photosystem II antenna assembly

Wenming Tian [b,c], Jun Chen [a,*], Liezheng Deng [b,*], Mingdong Yao [a], Heping Yang [b], Yang Zheng [a], Rongrong Cui [b], Guohe Sha [b]

[a] Dalian National Laboratory for Clean Energy, Dalian Institute of Chemical Physics, Chinese Academy of Sciences, Dalian 116023, China
[b] State Key Laboratory of Molecular Reaction Dynamics, Dalian Institute of Chemical Physics, Chinese Academy of Sciences, Dalian 116023, China
[c] Graduate University of Chinese Academy of Sciences, Beijing 100049, China

ARTICLE INFO

Article history:
Received 13 September 2014
Received in revised form 28 October 2014
Accepted 24 November 2014
Available online 5 December 2014

Keywords:
Photosystem II
LHCII
Chlorophyll fluorescence
Non-photochemical quenching
Photoprotection
Energy relaxation

ABSTRACT

Plant photosystem II (PSII) is a multicomponent pigment-protein complex that harvests sunlight via pigments photoexcitation, and converts light energy into chemical energy. Against high light induced photodamage, excess light absorption of antenna pigments triggers the operation of photoprotection mechanism in plant PSII. Non-photochemical energy relaxation as a major photoprotection way is essentially correlated to the excess light absorption. Here we investigate the energy relaxation of plant PSII complexes with varying incident light density, by performing steady-state and transient chlorophyll fluorescence measurements of the grana membranes (called as BBY), functional moiety PSII reaction center and isolated light-harvesting complex LHCII under excess light irradiation. Based on the chlorophyll fluorescence decays of these samples, it is found that an irradiation density dependent energy relaxation occurs in the LHCII assemblies, especially in the antenna assembly of PSII supercomplexes in grana membrane, when irradiation increases to somewhat higher density levels. Correspondingly, the average chlorophyll fluorescence lifetime of the highly isolated BBY fragments gradually decreases from ~1680 to ~1360 ps with increasing the irradiation density from 6.1×10^9 to 5.5×10^{10} photon cm^{-2} $pulse^{-1}$. Analysis of the relation of fluorescence decay change to the aggregation extent of LHCIIs suggests that a dense arrangement of trimeric LHCIIs is likely the structural base for the occurrence of this irradiation density dependent energy relaxation. Once altering the irradiation density, this energy relaxation is quickly reversible, implying that it may play an important role in photoprotection of plant PSII.

1. Introduction

Photosystem II (PSII) is a multicomponent pigment-protein complex embedded in the thylakoid membranes of plant, algae, and cyanobacteria, that harvests sunlight with pigments to drive the reactions of water oxidation and plastoquinone reduction [1,2]. The architecture of plant PSII supercomplexes have been identified by single particle electron microscopy [1,3,4], showing the location and orientation of their components which include the light-harvesting antenna proteins and the reaction core complex. The outer light-harvesting antenna consists of trimeric complexes LHCII and monomeric complexes CP24, CP26 and CP29. The crystal structure of LHCII from spinach distinguishes in each monomer that 8 Chl a, 6 Chl b and 4 carotenoid pigment molecules are confined in specific sites associated with the polypeptides [5]. Beside, spinach CP29 contains 13 Chl and 3 carotenoid pigment molecules [6]. In addition, 35 Chls in a cyanobacteria PSII core complex are confirmed by resolving its crystal structure [7].

These light-harvesting antenna systems collect the excitation energy and efficiently transfer it to the reaction center (RC) under irradiation at low light levels. Under excess light irradiation, the speed of the energy absorption exceeds the turnover frequency of the PSII reaction center, that could induce photodamage in reaction carriers and protein structure due to photo-oxidative stress [8–12]. To prevent permanent damages to photosynthetic apparatus, PSII switches on photoprotective mechanisms, one is called as non-photochemical quenching (NPQ) in which excess energy is dissipated as heat [13–15]. As known to date, heterogeneous processes are involved in NPQ. One predominant, rapidly relaxing contribution to NPQ is called as energy dependent quenching or qE, which can be triggered by proton gradient across thylakoid membrane and reversible with relaxation in seconds to minutes [16,17], and in which PsbS protein [18] and zeaxanthin [19] are found to play important roles. Another contribution to NPQ, qT, is attributed to state transition with the dissociation of LHCs [20]. In addition, a slowly relaxing

Abbreviations: Chl, chlorophyll; PSII, Photosystem II; RC, reaction center; DA-LHCII, deeply aggregated LHCII; SA-LHCII, slightly aggregated LHCII; NPQ, non-photochemical quenching; SDS-PAGE, sodium dodecyl sulfate polyacrylamide gel electrophoresis; MES, 4-Morpholineethanesulfonic acid; OGP, octylglucopyranoside

* Corresponding authors.
E-mail addresses: junchen@dicp.ac.cn (J. Chen), dlz@dicp.ac.cn (L. Deng).

http://dx.doi.org/10.1016/j.bbabio.2014.11.010
0005-2728/

contribution to NPQ, qI, is related to photoinhibition quenching of photosynthesis. However, due to intricate pigment distribution, delicate interactions between each components, and concerted kinetic regulation, the detailed mechanisms of NPQ are still under debated.

Different mechanisms focusing on the quenching sites have been evidenced to elaborate the NPQ processes related to LHCII [21–26]. One of the LHCII-bound luteins, Lut1, is indicated as a trap site accepting energy transfer from the neighboring Chl [21,22]. The configuration twist of the neoxanthin is suggested to open a channel for energy dissipation from Chl a to the low-lying excited state of Lut1 [21]. It is reported that light-induced isomerization of the LHCII-bound neoxanthin leads to formation of LHCII supramolecular structures creating energy quenching sites associated with the peripheral Chl molecules [27]. On the lumenal side, the conformational changes in the loop region associated with Lut2 are likely involved in quenching the triplet Chl [26]. Besides, researches show that the aggregation of LHCII brings about the formation of efficient quenching site contributing to NPQ [28–36].

Actually, the incident light density is one of the key factors to probe NPQ process. qE and photoinactivation can be enhanced with increasing the incident light density [37]. Moreover, NPQ value is irradiation density dependent [38]. However, not much attention has been paid on the relation of energy relaxation kinetics of PSII to irradiation density, especially for plant PSII supercomplexes which are the main constituent of grana membrane. In this work, we investigate the energy relaxation of plant grana membrane by monitoring Chl fluorescence decays with altering the irradiation density. Analysis is also conducted, on the basis of the steady-state and transient fluorescence measurements of grana membrane, functional moiety PSII RC and isolated LHCII under excess light irradiation, to get insight into an irradiation density dependent energy relaxation of PSII supercomplexes.

2. Materials and methods

2.1. Sample preparation

The PSII membrane fragments (referred to as BBY) from fresh spinach leaves were prepared as described previously [39,40]. The isolated BBY was finally suspended in SMN buffer (50 mM MES, 400 mM sucrose, 15 mM NaCl, pH 6.0) at Chl concentration of 2.4 mg mL^{-1}, and then stored at −70 °C until use. The O_2 evolution rates of these BBY samples were over 800 μmol O_2 (mg of Chl)$^{-1}$ h^{-1} when 2,6-dichloro-*p*-benzoquinone and potassium ferricyanide were used as exogenous electron acceptor.

RC complexes were also isolated from fresh spinach leaves and purified as described previously [41]. Non-ionic detergent n-octyl-β-D-thioglucoside was used to separate RC from PSII membrane. The isolated RC was finally suspended in a SMN buffer (50 mM MES, 400 mM sucrose, 15 mM NaCl, pH 6.0) at concentration of 0.3 mg Chl mL^{-1}, and then stored at −70 °C until use. The O_2 evolution rates of these RC samples were over 1100 μmol O_2 (mg of Chl)$^{-1}$ h^{-1}.

LHCII from spinach was isolated through a sucrose gradient as described previously [42], and solved in a buffer (25 mM MES, 15 mM NaCl, 5 mM $CaCl_2$, 10% sucrose, 60 mM octylglucopyranoside (OGP), pH 6.0) at concentration of 0.4 mg Chl mL^{-1}. The aggregated LHCII was prepared via detergent removal by dialysis, against above buffer without detergent OGP and $CaCl_2$, at 4 °C overnight.

2.2. SDS-PAGE

The samples were denatured in the aqueous solution (6.0 M urea, 5% SDS, 125 mM dithiothreitol, 104 mM Na_2CO_3 and 0.08% bromophenol blue) for 1 h at room temperature. The denatured samples were subjected to a urea-polyacrylamide gel, where the stacking layer contained 6% acrylamide and the resolving layer contained 15% acrylamide. The SDS-PAGE was run at 100 V until samples had completely entered the stacking gel, and then run at 150 V for about 4 h. The gel was stained with 0.05% Coomassie brilliant blue R-250 for 1 h, and then destained overnight with a 5% methanol and 10% acetic acid aqueous solution.

2.3. Fluorescence measurement

Transient fluorescence measurements were performed using laser scanning confocal fluorescence lifetime imaging microscopy (LCS-FLIM) combined with time-correlated single photon counting (DCS120 system, B&H, Germany; IX81 microscope, Olympus, Japan). Excitation of the sample was achieved with a laser of 405 nm wavelength, 80 MHz repetition rate, and ~100 ps pulse width. The laser spot on the sample was about 23 μm in diameter. The laser intensity at samples was adjusted by a neutral density filter from 100 to 9000 nW (measured with a power meter, PM100D S130VC, Thorlabs, USA), corresponding to the irradiation density from 6.1×10^8 to 5.5×10^{10} photon cm^{-2} $pulse^{-1}$. The laser scanning area on samples was around 2 mm × 2 mm. Each scanning contained 256 × 256 pixels with the laser dwell time of 6.4 μs in each pixel, and the whole acquisition time of 10 repetitions was around 5 seconds. The data were the average of output from all the pixels. The transient fluorescence signal in the range 600–900 nm was collected using a high speed detector (HPM-100-50, Hamamatsu, Japan). The instrument response function of this system is approximately 200 ps. For lifetime analysis, the software SPC Image (B&H) was used. The quality of the data fitting was judged by the parameter χ^2 and the residual. To obtain steady-state fluorescence emission spectra, a setup which mainly consists of a monochromator (SpectraPro-2300i, Acton Research Co., USA) and an intensified charge coupled device (ICCD) camera (PI-MAX:1024HB, USA) was coupled to the excitation part of above transient system, sharing the same excitation source and microscope objective for signal collection. All measurements were carried out at room temperature.

For sampling, a small volume of sample (~25 μL) was placed in a quartz cuvette with optical length of 0.1 mm. Prior to fluorescence measurements, the samples were kept at room temperature in the dark for 30 min. To ensure the PSII complexes were in closed RC state, the samples were then exposed to a red light (610–720 nm, from a halogen lamp) with intensity of 2.5×10^{-3} mW cm^{-2} for one minute, and this red light illumination was keeping on or off during the fluorescence measurements. The interference of this red light on the fluorescence signal measurements was confirmed to be negligible.

3. Results

3.1. Steady-state fluorescence spectra of the BBY and RC samples

Fig. 1 shows the polypeptide compositions of the BBY, RC and LHCII samples by SDS-PAGE. Compared to BBY, no LHCII remains on the RC sample which contains polypeptide D1, D2, CP43, CP47 and PsbO. The LHCII sample is mainly in trimeric conformation based on the mass separation by sucrose gradient.

The steady-state fluorescence spectra of the BBY, RC and LHCII samples with a low concentration (50 μg Chl mL^{-1}) have been measured at room temperature (see Fig. 2). The BBY, RC and LHCII samples all exhibit a main fluorescence band with a peak at 683, 682, and 681 nm, respectively, and a broad shoulder band at around 740 nm. These fluorescence bands are attributed to the radiative relaxation of excited Chl [43,44]. The shoulder band is assigned to the vibronic mode of Chl [45,46].

In addition, we investigated the relative fluorescence emission intensity of BBY and RC samples with a close monomer concentration. For plant PSII membrane, by HPLC chromatography detected ~274 Chls per PSII monomer [47]. Whereas, 35 Chls are bound in the reaction center complex according to its crystal structure from a cyanobacteria [7]. To ensure the proteins fully covering the imaging field, a high concentration of BBY sample (2.4 mg Chl mL^{-1}) and a RC sample (0.3 mg Chl mL^{-1}) with the close monomer concentration were adopted. In accordance with the Chl concentration analysis, the BBY sample gives much stronger fluorescence than the RC sample, as shown in figure S1.

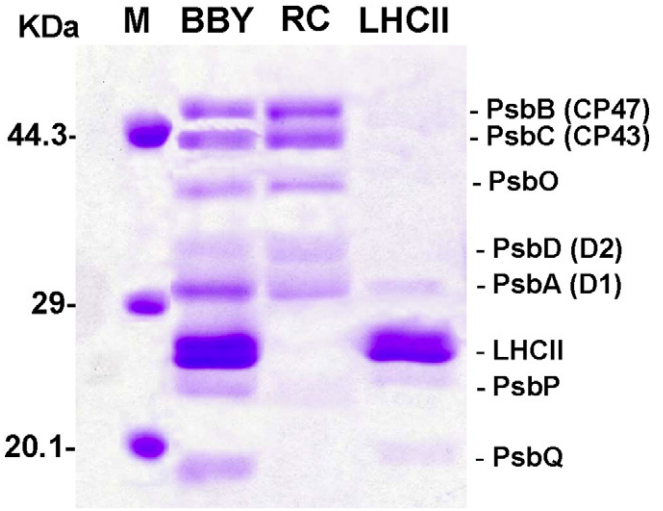

Fig. 1. SDS-PAGE patterns of BBY, RC and LHCII samples from spinach. The protein standards are labeled with molecular weights on the left. The injected amounts of the BBY, RC and LHCII samples on the gel were 4.0, 0.5 and 4.0 μg Chl, respectively. The polypeptide compositions are indicated on the right side.

The effect of incident light density on the fluorescence emission spectra was further investigated. The BBY sample was diluted to 50 μg Chl mL^{-1}. As shown by the bright field images (Fig. 3a, figure S2), a good dispersion of the membrane fragments was achieved at this concentration. To obtain the steady-state fluorescence spectra with avoiding the influence of re-absorption, each spectrum was measured by parking the laser beam at isolated membrane fragments, and the spectra shown in Fig. 3b represent the average of twenty data sets from different membrane fragments. As a result, the steady-state fluorescence spectra (Fig. 3b) of the BBY sample exhibit a strongest band with a peak at 683 nm and a broad shoulder band at around 740 nm. However, these bands do not show a change in frequency with increasing the irradiation density from 6.1×10^8 to 5.5×10^{10} photon cm^{-2} $pulse^{-1}$.

3.2. Transient fluorescence analysis of the BBY, RC and LHCII samples

The analysis of the transient fluorescence behaviors of the samples has been performed. The fluorescence signal in the range of

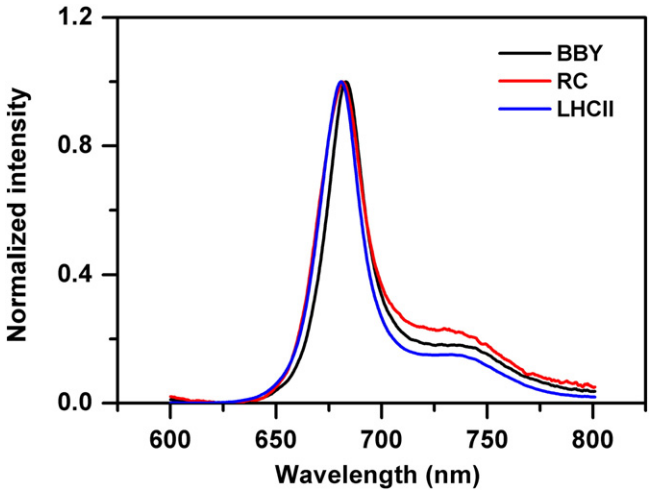

Fig. 2. Steady-state fluorescence spectra of the BBY (black line), RC (red line) and LHCII (blue line) samples. The concentrations of these samples were all 50 μg Chl mL^{-1}. These samples were kept at room temperature in darkness for 30 min before fluorescence measurements. The irradiation density was 5.5×10^{10} photon cm^{-2} $pulse^{-1}$. These spectra were normalized at the maximum emission intensity.

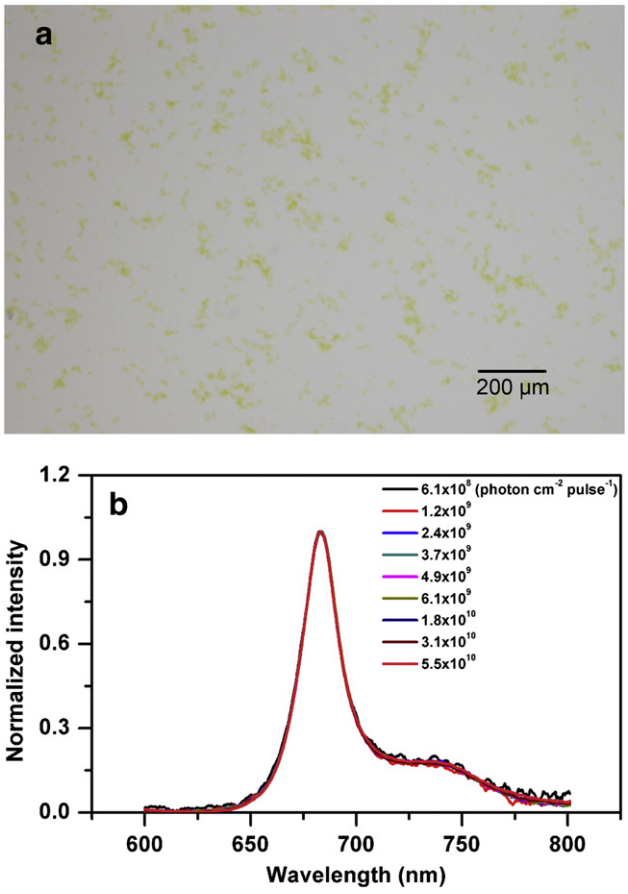

Fig. 3. (a) Bright field image and (b) steady-state fluorescence spectra of a BBY sample. The steady-state fluorescence spectra were obtained at different excitation densities, and represent the average of twenty data sets. These spectra were normalized at the maximum emission intensity. The concentration of the BBY sample was 50 μg Chl mL^{-1}.

600–900 nm was collected and analyzed using the software SPC Image (B&H). The quality of fitting was checked by the reduced chi-square (χ^2) criterion and the residual. All the decay traces were fitted by single exponential component, because the χ^2 value and the residual did not get better by increasing the fitting exponent (see figure S3 and Table S1). The fluorescence lifetime also represents the average of all fluorescence decays in the imaging field.

In order to explore the photoprotection mechanism under excess light irradiation, we focused on the PSII complexes with closed RC state which is formed by a continuous-wave red light illumination of 2.5×10^{-3} mW cm^{-2}. The transient fluorescence decay of BBY is traced by changing the irradiation density between 6.1×10^8 and 5.5×10^{10} photon cm^{-2} $pulse^{-1}$. Shown in Fig. 4a, in the range of irradiation density from 6.1×10^8 to 6.1×10^9 photon cm^{-2} $pulse^{-1}$, the fluorescence lifetime of BBY slightly decreases from ~1750 to ~1680 ps. These lifetime values are in accordance with the average maximum lifetime (not exceed 2 ns) arised from the closed state of PSII as reported previously [35][48–51]. If the irradiation density is increased far beyond 6.1×10^9 photon cm^{-2} $pulse^{-1}$, the fluorescence lifetime of BBY decreases almost linearly with increasing the irradiation density (Fig. 4b). At 5.5×10^{10} photon cm^{-2} $pulse^{-1}$, the lifetime goes down to 1360 ps, ~320 ps less than that at 6.1×10^9 photon cm^{-2} $pulse^{-1}$. This fluorescence behavior indicates that a different energy regulation turns on at high excitation levels. Interestingly, we found that this change in fluorescence lifetime is quickly reversible with decreasing the irradiation density. This illustrates that this energy regulation is recoverable, not due to a destructive impact on the protein.

In order to find out which part of the PSII complex is responsible for this energy regulation, the transient fluorescence behavior of RC

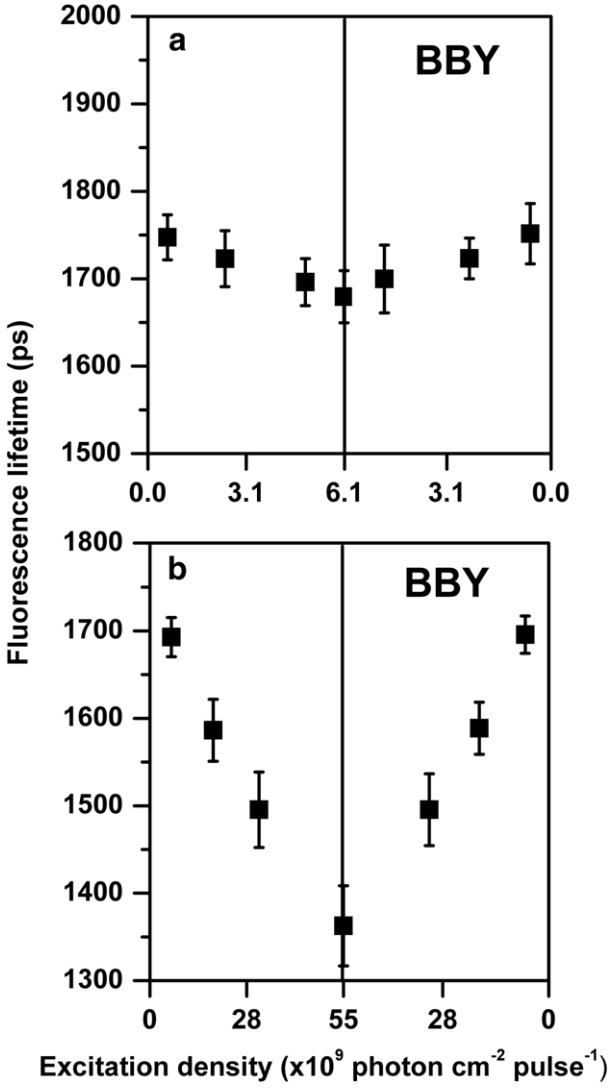

Fig. 4. The fluorescence lifetime of the BBY versus the irradiation density (a) between 6.1×10^8 and 6.1×10^9 photon cm^{-2} $pulse^{-1}$, and (b) between 6.1×10^9 and 5.5×10^{10} photon cm^{-2} $pulse^{-1}$. Along with the fluorescence measurements, the irradiation density was step by step increased to certain level, and then decreased backwards. During the fluorescence measurements, the red light illumination of 2.5×10^{-3} mW cm^{-2} was keeping onto the samples to make sure they are in closed RC state. The concentration of this BBY sample was 50 μg Chl mL^{-1}. The data shown represent the averages of ten independent experiments with standard deviation.

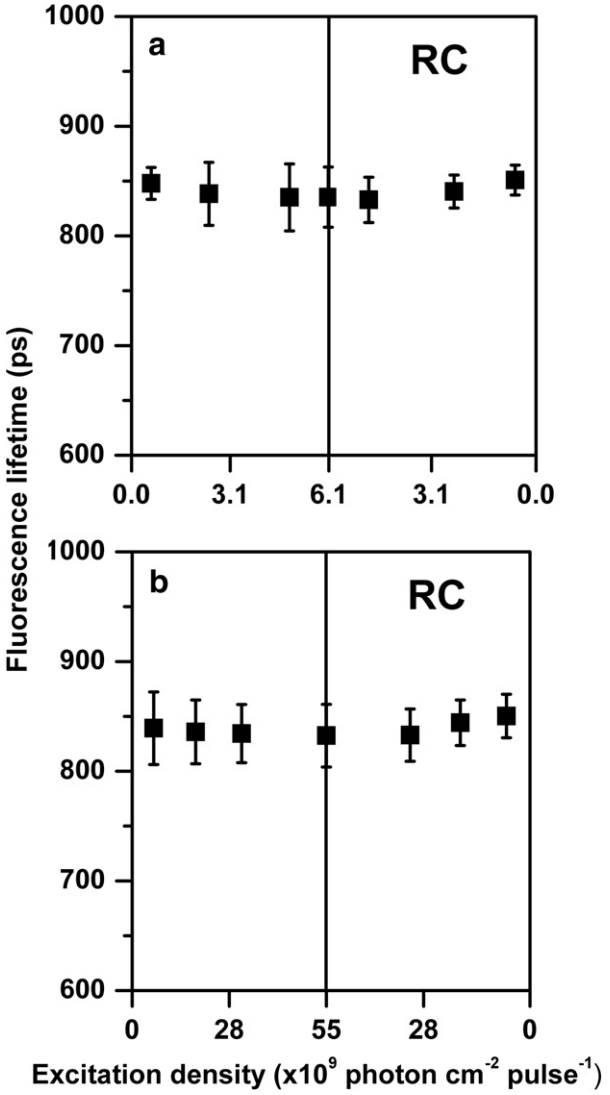

Fig. 5. The fluorescence lifetime of the RC complex versus the irradiation density (a) between 6.1×10^8 and 6.1×10^9 photon cm^{-2} $pulse^{-1}$, and (b) between 6.1×10^9 and 5.5×10^{10} photon cm^{-2} $pulse^{-1}$. Along with the fluorescence measurements, the irradiation density was step by step increased to certain level, and then decreased backwards. During the fluorescence measurements, the red light illumination of 2.5×10^{-3} mW cm^{-2} was keeping onto the samples to make sure they are in closed RC state. The concentration of this RC complex sample was 50 μg Chl mL^{-1}. The data shown represent the averages of ten independent experiments with standard deviation.

complex with altering the irradiation density was also traced (Fig. 5). Results showed that the fluorescence lifetime of RC remains unchanged (~840 ps) with increasing the irradiation density even up to 5.5×10^{10} photon cm^{-2} $pulse^{-1}$. This demonstrates that the energy regulation detected in BBY at high excitation levels (Fig. 4b) does not take place in the RC complex. Therefore, it is likely attributed to the outer light-harvesting antenna of PSII.

We also investigated the transient fluorescence behavior of isolated LHCII. Shown in Fig. 6a, the fluorescence lifetime of the LHCII sample is detected to be 3130 ± 17 ps and is nearly unchanged at low excitation levels. However, irradiation with higher density induces a decrease in the fluorescence lifetime of LHCII (Fig. 6b, the fit χ^2 shown in table S2). With increasing the irradiation density up to 5.5×10^{10} photon cm^{-2} $pulse^{-1}$, the fluorescence lifetime of LHCII gradually decreases down to 3070 ± 13 ps. Thus, these results demonstrate that an energy regulation can be triggered in the LHCII under excess irradiation.

3.3. Steady-state and transient fluorescence analysis of the aggregated LHCII samples

About the origins of the Chl fluorescence quenching in LHCII, it is reported that the aggregation of LHCIIs each other leads to a huge drop in the Chl fluorescence lifetime along with a red shift of the main fluorescence band [33,36]. The lifetime of ~3130 ps (Fig. 6a) for the LHCII sample could be correlated to a status of slight aggregation [35]. Further, we conducted similar fluorescence measurements to a deeply aggregated LHCII (DA-LHCII) sample, which was prepared by dialyzing the detergent out. As shown in figure S4, the aggregation is obvious for this LHCII sample. For the steady-state fluorescence emission (Fig. 7), a red shift of 47 cm^{-1} (2.2 nm) was detected for the DA-LHCII compared with the slightly aggregated LHCII (SA-LHCII). On the other hand, the fluorescence lifetime of the DA-LHCII at a low irradiation density (Fig. 8a) drops down to ~830 ps, ~2300 ps faster than that of the SA-LHCII. However, the change in the fluorescence lifetime of the

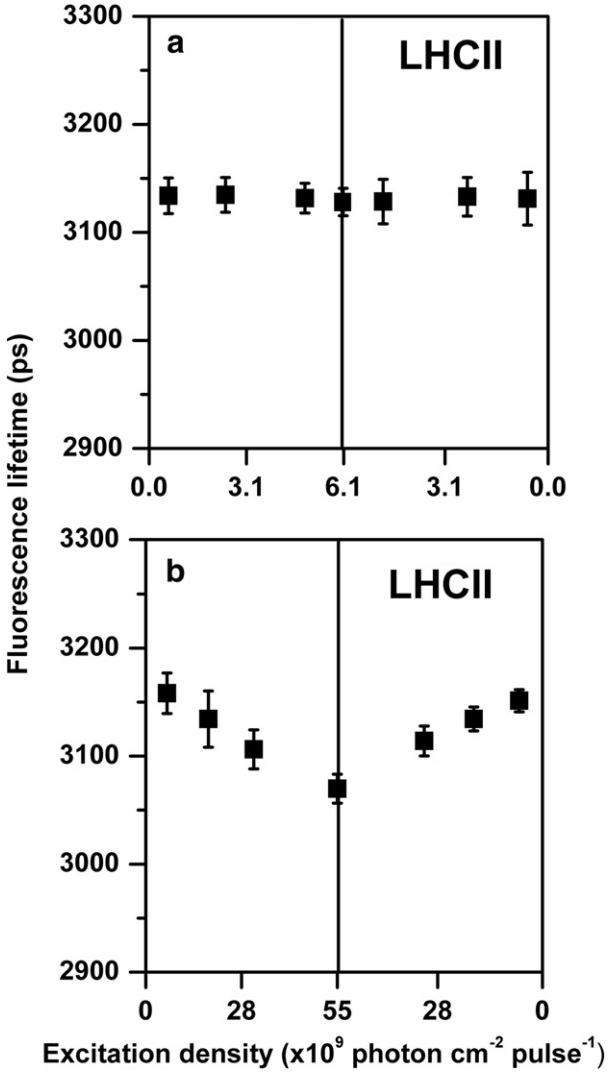

Fig. 6. The fluorescence lifetime of the LHCII versus the irradiation density (a) between 6.1×10^8 and 6.1×10^9 photon cm^{-2} $pulse^{-1}$, and (b) between 6.1×10^9 and 5.5×10^{10} photon cm^{-2} $pulse^{-1}$. Along with the fluorescence measurements, the irradiation density was step by step increased to certain level, and then decreased backwards. No red light illumination was keeping onto the samples. The concentration of this LHCII sample was 50 μg Chl mL^{-1}. The data shown represent the averages of ten independent experiments with standard deviation.

DA-LHCII with increasing the irradiation density (Fig. 8b) exists in a similar way to the SA-LHCII and to BBY.

3.4. Fluorescence of BBY with a high concentration

In contrast with the BBY sample with a low concentration (50 μg Chl mL^{-1}), the dense BBY sample (2.4 mg Chl mL^{-1}) presents a red shift in the strongest fluorescence emission band, as shown in Fig. 9. This phenomenon is probably due to the fluorescence re-adsorption effect [52].

Meanwhile, the transient fluorescence of this dense BBY sample was also traced. Shown in Fig. 10, this sample presents a slight decrease of fluorescence lifetime with increasing the irradiation density from 6.1×10^8 to 6.1×10^9 photon cm^{-2} $pulse^{-1}$, and a big decrease of fluorescence lifetime from ~1800 to ~1430 ps with increasing the irradiation density from 6.1×10^9 to 5.5×10^{10} photon cm^{-2} $pulse^{-1}$. This decay behavior of the dense BBY fragments is similar to that of the highly isolated BBY fragments.

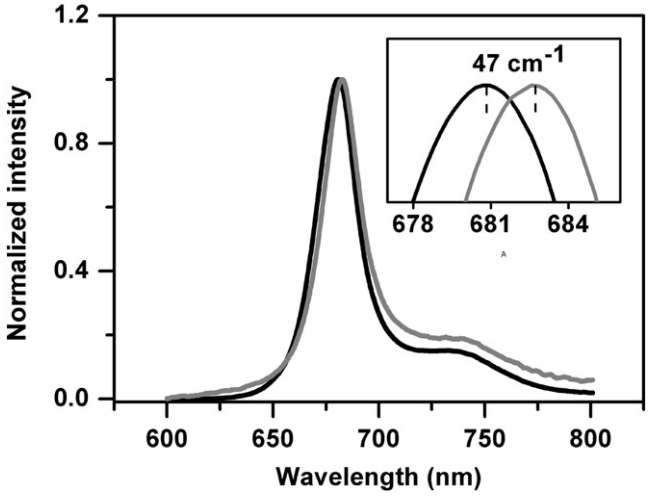

Fig. 7. Steady-state fluorescence spectra of the slightly aggregated LHCII (black line) and deeply aggregated LHCII (gray line) at the irradiation density of 5.5×10^{10} photon cm^{-2} $pulse^{-1}$. Spectra with normalized intensity at maximum are shown. The inset zooms in the peak region and marks the spectral shift.

4. Discussion

In this work, we observed that the nanosecond-order fluorescence lifetime for BBY and for isolated LHCII decreases with increasing irradiation density to somewhat higher levels (Figs. 4b, 6b). However, the fluorescence lifetime of RC complex remains unchanged under the same conditions. These results demonstrate that an irradiation density dependent energy relaxation occurs in association with the component LHCII of plant PSII membrane. We also found that this energy regulation process is quickly reversible upon decreasing irradiation density. Similarly, Jennings et al. showed that during the light induced fluorescence quenching kinetics (in the second time domain) the overall fluorescence lifetime of the illuminated LHCII sample decreases in the nanosecond time domain [28,32].

To date, many researches demonstrate that a part of NPQ for plant PSII occurs in the outer antenna [22,25,53,54]. Numbers of reports point out the LHCII aggregation-induced fluorescence quenching, that is always accompanied with a red shift in the Chl fluorescence band (~683 nm) [22,31,34,35]. The aggregation of trimeric LHCII causing conformational changes was suggested to form an energy transfer pathway for Chl-excited state deactivation via Chl/Chl exciton pairs [23,34,55], or through the S1 state of a carotenoid [21,56]. Similarly, we observed the aggregation of isolated LHCIIs giving rise to a drastic decrease in fluorescence lifetime from ~3130 ps down to ~830 ps (Figs. 6, 8). Correspondingly, a spectral red shift (47 cm^{-1}) of the Chl main fluorescence band for the DA-LHCII compared with the SA-LHCII was detected as shown in Fig. 7.

However, not only the BBY samples but also the DA-LHCII sample presents an approximately linear decrease in fluorescence lifetime with increasing the irradiation density from 6.1×10^9 to 5.5×10^{10} photon cm^{-2} $pulse^{-1}$ (Figs. 4b, 8b and 10b), and these decay changes are quickly reversible once reducing the irradiation density. In addition, the normalized steady-state fluorescence spectra of the BBY with increasing irradiation density from 6.1×10^8 to 5.5×10^{10} photon cm^{-2} $pulse^{-1}$ do not exhibit a frequency shift in the Chl main fluorescence band (Fig. 3). Therefore, these results indicate that the mechanism of this irradiation density dependent fluorescence quenching is not related to the red shift of the Chl main fluorescence band.

Analysis of the fluorescence decay with increasing the irradiation density from 6.1×10^9 to 5.5×10^{10} photon cm^{-2} $pulse^{-1}$ shows a 3% drop in fluorescence lifetime for the SA-LHCII, 11% for the DA-LHCII and 20% for the BBY. This analysis suggests that a dense arrangement

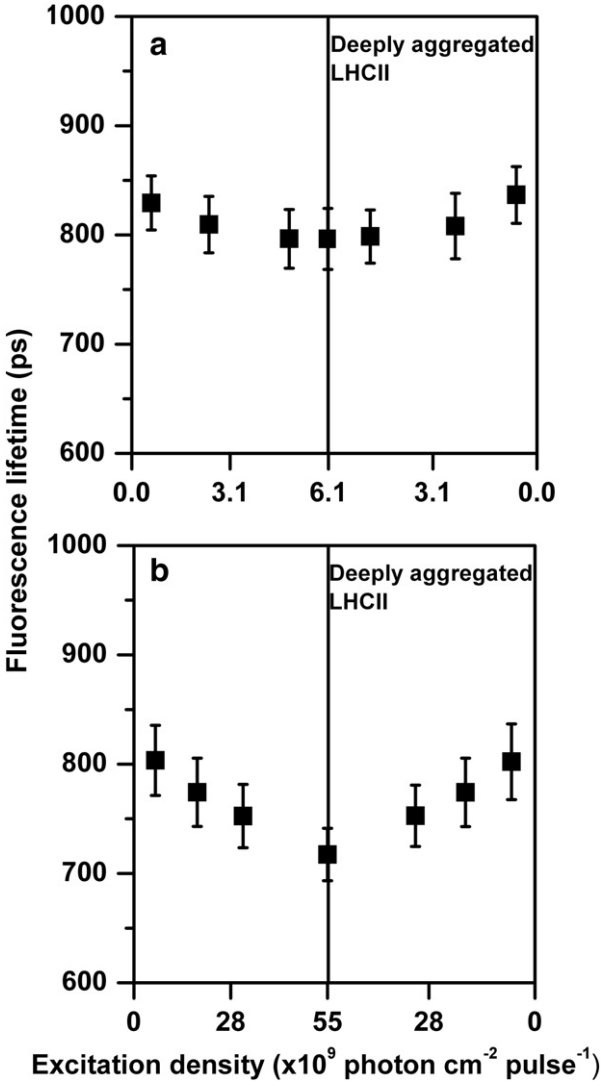

Fig. 8. The fluorescence lifetime of the DA-LHCII versus the irradiation density (a) between 6.1×10^8 and 6.1×10^9 photon cm^{-2} $pulse^{-1}$, and (b) between 6.1×10^9 and 5.5×10^{10} photon cm^{-2} $pulse^{-1}$. Along with the fluorescence measurements, the irradiation density was step by step increased to certain level, and then decreased backwards. No red light illumination was keeping onto the samples. The concentration of this DA-LHCII was 50 μg Chl mL^{-1}. The data shown represent the averages of ten independent experiments with standard deviation.

of LHCII is likely the structural base for the occurrence of this irradiation density dependent fluorescence quenching. Especially for BBY, PSII supercomplexes are crowded together, occupying almost ~80% area in grana thylakoid [57–59]. The most populated protein subunit of PSII supercomplexes is LHCII [60]. This means that LHCII is densely arranged in BBY. Compared to the random aggregated DA-LHCII sample with 11% drop in fluorescence lifetime, the proposed non-random structured organization of PSII supercomplexes for BBY [58] is probably a positive factor affecting the irradiation density dependent fluorescence quenching.

By comparing the steady-state fluorescence spectra of the BBY samples with different concentrations, a red shift of the Chl main fluorescence band (peak at 687 nm) and an increase of the vibronic shoulder band (at around 740 nm) for a dense BBY sample of 2.4 mg Chl mL^{-1} was observed (Fig. 9). This spectral behavior can be explained to the re-absorption effect on a dense sample. On the other hand, for this dense BBY sample, a small and progressive red shift of the fluorescence maximum is detected as a function of the irradiation density (see figure S5). Moreover, the relative contribution of the vibronic red shoulder

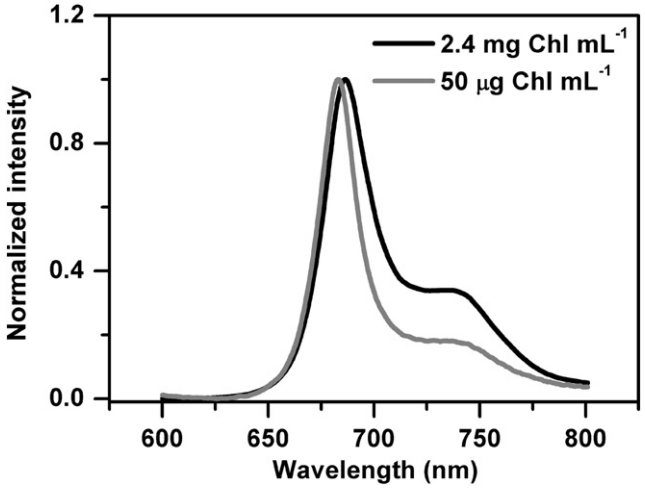

Fig. 9. Normalized steady-state fluorescence spectra of BBY with the concentration of 50 μg Chl mL^{-1} (gray line) and 2.4 mg Chl mL^{-1} (black line) at the irradiation density of 5.5×10^{10} photon cm^{-2} $pulse^{-1}$.

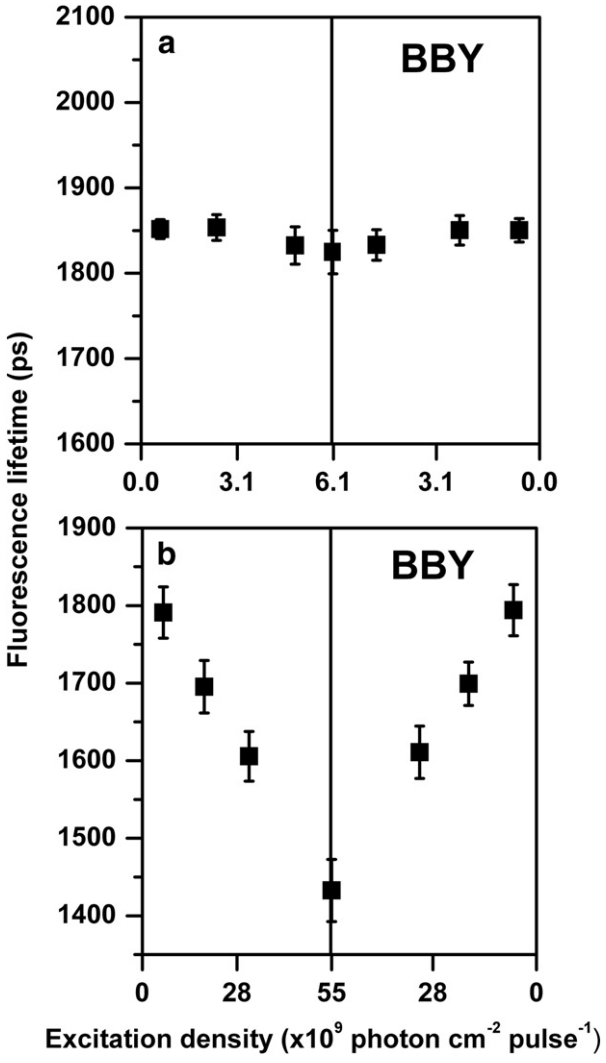

Fig. 10. The fluorescence lifetime of the BBY (2.4 mg Chl mL^{-1}) versus the irradiation density (a) between 6.1×10^8 and 6.1×10^9 photon cm^{-2} $pulse^{-1}$, and (b) between 6.1×10^9 and 5.5×10^{10} photon cm^{-2} $pulse^{-1}$. Along with the fluorescence measurements, the irradiation density was step by step increased to certain level, and then decreased backwards. During the fluorescence measurement, the red light illumination of 2.5×10^{-3} mW cm^{-2} was keeping onto the samples to make sure they are in closed RC state. The data shown represent the averages of five independent experiments with standard deviation.

increases. These two concomitant effects can be also explained in terms of fluorescence re-absorption due to a different penetration of the exciting light (roughly proportional to the incident intensity) in the concentrated sample that increase the re-absorption effect in the measurement setup. However, the re-absorption effect seems not to influence the change in the fluorescence decay of the BBY with increasing the irradiation density (Figs. 4, 10). A 20% drop of fluorescence lifetime was estimated for both the highly isolated BBY sample and the dense BBY sample. Similarly, it is demonstrated that re-absorption of Chl fluorescence does not affect the picosecond-order fluorescence decay of leaves [52]. According to the fluorescence re-absorption phenomenon of the dense BBY sample, the possibility that the red shift of the Chl main fluorescence band of the DA-LHCII vs SA-LHCII can be due to the higher local concentration (figure S4) of Chl in the DA-LHCII sample that cause re-absorption cannot be ruled out. This comparison implies that a drastic decrease in the fluorescence lifetime of the DA-LHCII vs SA-LHCII is likely not related to the red shift of the Chl main fluorescence band.

On the other hand, researches on the Chl fluorescence of isolated LHCII found that ultrafast laser pulse with high density (usually exceed 1×10^{13} photon cm^{-2} $pulse^{-1}$) can induce singlet-singlet annihilation for the excited Chl in trimeric LHCII [61,62]. The singlet-singlet annihilation rate was determined to be (dozens of picoseconds)$^{-1}$ [62,63],this relative fast annihilation rate leads to a huge drop in the Chl fluorescence lifetime and intensity for LHCII. However, under our experimental conditions, the Chl fluorescence intensity increases almost linearly with increasing the irradiation density (data not shown), indicating no Chl singlet-singlet annihilation occurred in the LHCII for these cases. In addition, if assuming the existence of Chl singlet-singlet annihilation, the annihilation rate was calculated to be ~2×10^{-11} ps^{-1} (see supplementary material and figure S6) by fitting the fluorescence decay trace of the BBY sample excited at 5.5×10^{10} photon cm^{-2} $pulse^{-1}$. This value, ~2×10^{-11} ps^{-1}, is obviously unreasonable and far deviates from the acceptable range of the Chl singlet-singlet annihilation rate [62,63]. Thus, Chl singlet-singlet annihilation is excluded as a factor resulting in the irradiation density dependent energy relaxation which was probed in our work.

In conclusion, the transient Chl fluorescence data provide evidence that an irradiation density dependent energy relaxation takes place in the LHCII assembly in plant PSII membrane. A dense arrangement of trimeric LHCIIs is likely required for effective occurrence of this irradiation density dependent energy relaxation. This energy relaxation is quickly reversible once altering the irradiation density, implying that it may play an important role in photoprotection of plant PSII.

Acknowledgements

Jun Chen acknowledges the 100 talent fund from the Chinese Academy of Sciences. This work was also financially supported by National Natural Science Foundation of China (31100618, 20603039, 21173217).

Appendix A. Supplementary data

Supplementary data to this article can be found online at http://dx.doi.org/10.1016/j.bbabio.2014.11.010.

References

[1] J.P. Dekker, E.J. Boekema, Supramolecular organization of thylakoid membraneproteins in green plants, Biochim. Biophys. Acta Bioenerg. 1706 (2005) 12–39.
[2] N. Nelson, C.F. Yocum, Structure and function of photosystems I and II, Annu. Rev. Plant Biol. 57 (2006) 521–565.
[3] S. Caffarri, R. Kouřil, S. Kereïche, E.J. Boekema, R. Croce, Functional architecture of higher plant photosystem II supercomplexes, EMBO J. 28 (2009) 3052–3063.
[4] R. Kouřil, J.P. Dekker, E.J. Boekema, Supramolecular organization of photosystem II in green plants, Biochim. Biophys. Acta Bioenerg. 1817 (2012) 2–12.
[5] Z.F. Liu, et al., Crystal structure of spinach major light-harvesting complex at 2.72 angstrom resolution, Nature 428 (2004) 287–292.
[6] X.W. Pan, et al., Structural insights into energy regulation of light-harvesting complex CP29 from spinach, Nat. Struct. Mol. Biol. 18 (2011) 309–315.
[7] Y. Umena, K. Kawakami, J.R. Shen, N. Kamiya, Crystal structure of oxygen-evolving photosystem II at a resolution of 1.9 angstrom, Nature 473 (2011) 55–61.
[8] A. Krieger-Liszkay, Singlet oxygen production in photosynthesis, J. Exp. Bot. 56 (2005) 337–346.
[9] N. Ohnishi, S.I. Allakhverdiev, S. Takahashi, S. Higashi, M. Watanabe, Y. Nishiyama, N. Murata, Two-step mechanism of photodamage to photosystem II: Step 1 occurs at the oxygen-evolving complex and step 2 occurs at the photochemical reaction center, Biochemistry 44 (2005) 8494–8499.
[10] P. Pospíšil, Production of reactive oxygen species by photosystem II, Biochim. Biophys. Acta Bioenerg. 1787 (2009) 1151–1160.
[11] V. Imre, Role of charge recombination processes in photodamage and photoprotection of the photosystem II complex, Physiol. Plant. 142 (2011) 6–16.
[12] S. Takahashi, M.R. Badger, Photoprotection in plants: A new light on photosystem II damage, Trends Plant Sci. 16 (2011) 53–60.
[13] P. Müller, X.P. Li, K.K. Niyogi, Non-photochemical quenching. A response to excess light energy, Plant Physiol. 125 (2001) 1558–1566.
[14] S. de Bianchi, M. Ballottari, L. Dall'Osto, R. Bassi, Regulation of plant light harvesting by thermal dissipation of excess energy, Biochem. Soc. Trans. 38 (2010) 651–660.
[15] D. Carbonera, C. Gerotto, B. Posocco, G.M. Giacometti, T. Morosinotto, NPQ activation reduces chlorophyll triplet state formation in the moss Physcomitrella patens, Biochim. Biophys. Acta Bioenerg. 1817 (2012) 1608–1615.
[16] G.H. Krause, C. Vernotte, J.M. Briantais, Photonduced quenching of chlorophyll fluorescence in intact chloroplasts and alga-resulation into 2 components, Biochim. Biophys. Acta 679 (1982) 116–124.
[17] J. Zaks, K. Amarnath, E.J. Sylak-Glassman, G.R. Fleming, Models and measurements of energy-dependent quenching, Photosynth. Res. 116 (2013) 389–409.
[18] X.P. Li, O. Bjorkman, C. Shih, A.R. Grossman, M. Rosenquist, S. Jansson, K.K. Niyogi, A pigment-binding protein essential for regulation of photosynthetic light harvesting, Nature 403 (2000) 391–395.
[19] P. Jahns, A.R. Holzwarth, The role of the xanthophyll cycle and of lutein in photoprotection of photosystem II, Biochim. Biophys. Acta Bioenerg. 1817 (2012) 182–193.
[20] M. Iwai, M. Yokono, N. Inada, J. Minagawa, Live-cell imaging of photosystem II antenna dissociation during state transitions, Proc. Natl. Acad. Sci. U. S. A. 107 (2010) 2337–2342.
[21] A.V. Ruban, et al., Identification of a mechanism of photoprotective energy dissipation in higher plants, Nature 450 (2007) 575–579.
[22] M.P. Johnson, A.V. Ruban, Photoprotective energy dissipation in higher plants involves alteration of the excited state energy of the emitting chlorophyll(s) in the light harvesting antenna II (LHCII), J. Biol. Chem. 284 (2009) 23592–23601.
[23] M.G. Mueller, P. Lambrev, M. Reus, E. Wientjes, R. Croce, A.R. Holzwarth, Singlet energy dissipation in the photosystem II light-harvesting complex does not involve energy transfer to carotenoids, ChemPhysChem 11 (2010) 1289–1296.
[24] M. Zubik, et al., The negative feedback molecular mechanism which regulates excitation level in the plant photosynthetic complex LHCII: Towards identification of the energy dissipative state, Biochim. Biophys. Acta Bioenerg. 1827 (2013) 355–364.
[25] L. Wilk, M. Grunwald, P.N. Liao, P.J. Walla, W. Kühlbrandt, Direct interaction of the major light-harvesting complex II and PsbS in nonphotochemical quenching, Proc. Natl. Acad. Sci. U. S. A. 110 (2013) 5452–5456.
[26] L. Zhang, T.B. Melø, H. Li, K.R. Naqvi, C.H. Yang, The inter-monomer interface of the major light-harvesting chlorophyll a/b complexes of photosystem II (LHCII) influences the chlorophyll triplet distribution, J. Plant Physiol. 171 (2014) 42–48.
[27] M. Zubik, et al., Light-induced isomerization of the LHCII-bound xanthophyll neoxanthin: Possible implications for photoprotection in plants, Biochim. Biophys. Acta Bioenerg. 1807 (2011) 1237–1243.
[28] R.C. Jennings, F.M. Garlaschi, G. Zucchelli, Light-induced fluorescence quenching in the light-harvesting chlorophyll a/b protein complex, Photosynth. Res. 27 (1991) 57–64.
[29] R.C. Jennings, G. Zucchelli, R. Bassi, A. Vianelli, F.M. Garlaschi, The relation between the minor chlorophyll spectral forms and fluorescence quenching in aggregated light harvesting chlorophyll a/b complexII, Biochim. Biophys. Acta Bioenerg. 1184 (1994) 279–283.
[30] V. Barzda, L. Valkunas, G. Garab, Two independent mechanisms of fluorescence quenching in LHCII, Prog. Biophys. Mol. Biol. 65 (1996) (PE208-PE208).
[31] S. Vasil'ev, K.D. Irrgang, T. Schrötter, A. Bergmann, H.J. Eichler, G. Renger, Quenching of chlorophyll alpha fluorescence in the aggregates of LHCII: Steady state fluorescence and picosecond relaxation kinetics, Biochemistry 36 (1997) 7503–7512.
[32] V. Barzda, R.C. Jennings, G. Zucchelli, G. Garab, Kinetic analysis of the light-induced fluorescence quenching in light-harvesting chlorophyll a/b pigment-protein complex of photosystem II, Photochem. Photobiol. 70 (1999) 751–759.
[33] B. van Oort, A. van Hoek, A.V. Ruban, H. van Amerongen, Aggregation of light-harvesting complex II leads to formation of efficient excitation energy traps in monomeric and trimeric complexes, FEBS Lett. 581 (2007) 3528–3532.
[34] Y. Miloslavina, et al., Far-red fluorescence: A direct spectroscopic marker for LHCII oligomer formation in non-photochemical quenching, FEBS Lett. 582 (2008) 3625–3631.
[35] E. Belgio, M.P. Johnson, S. Jurić, A.V. Ruban, Higher plant photosystem II light-harvesting antenna, not the reaction center, determines the excited-state lifetime-both the maximum and the nonphotochemically quenched, Biophys. J. 102 (2012) 2761–2771.
[36] N.M. Magdaong, M.M. Enriquez, A.M. LaFountain, L. Rafka, H.A. Frank, Effect of protein aggregation on the spectroscopic properties and excited state kinetics of the LHCII pigment-protein complex from green plants, Photosynth. Res. 118 (2013) 259–276.

[37] T.J. Avenson, J.A. Cruz, D.M. Kramer, Modulation of energy-dependent quenching of excitons in antennae of higher plants, Proc. Natl. Acad. Sci. U. S. A. 101 (2004) 5530–5535.
[38] J. Serôdio, J. Lavaud, A model for describing the light response of the nonphotochemical quenching of chlorophyll fluorescence, Photosynth. Res. 108 (2011) 61–76.
[39] D.A. Berthold, G.T. Babcock, C.F. Yocum, A highly resolved, oxygen-evolving photosystem-II preparation from spinach thylakoid membranes-electron-paramagnetic-res and electron-transport properties, FEBS Lett. 134 (1981) 231–234.
[40] J. Chen, B.A. Barry, Ultraviolet resonance Raman microprobe spectroscopy of photosystem II, Photochem. Photobiol. 84 (2008) 815–818.
[41] R.K. Mishra, D.F. Ghanotakis, Selective extraction of CP-26 and CP-29 proteins without affecting the binding of the extrinsic proteins (33, 23 and 17 KDa) and the DCMU sensitivity of a photosystem-II core complex, Photosynth. Res. 42 (1994) 37–42.
[42] M. Ikeuchi, M. Yuasa, Y. Inoue, Simple and discrete isolation of an O-2-evolving PS-II reaction center complex retaining Mn and the extrinsic 33-KDa protein, FEBS Lett. 185 (1985) 316–322.
[43] R.C. Jennings, G. Zucchelli, F.M. Garlaschi, The influence of quenching by open reaction centers on the photosystem-II fluorescence emission-spectrum, Biochim. Biophys. Acta 1060 (1991) 245–250.
[44] D.O. Hall, K.K. Rao, Photosynthesis, sixthed, Cambridge University Press, Cambridge, 1999.
[45] H.K. Lichtenthaler, U. Rinderle, The role of chlorophyll fluorescence in the detection of stress conditions in plants, CRC Crit. Rev. Anal. Chem. 19 (1988) S29–S85.
[46] F. Franck, P. Juneau, R. Popovic, Resolution of the photosystem I and photosystem II contributions to chlorophyll fluorescence of intact leaves at room temperature, Biochim. Biophys. Acta Bioenerg. 1556 (2002) 239–246.
[47] J.S. Patzlaff, B.A. Barry, Pigment quantitation and analysis by HPLC reverse phase chromatography: A characterization of antenna size in oxygen-evolving photosystem II preparations from cyanobacteria and plants, Biochemistry 35 (1996) 7802–7811.
[48] M. Hodges, I. Moya, Time-resolved chlorophyll fluorescence studies of photosynthetic membranes: Resolution and characterization of four kinetic components, Biochim. Biophys. Acta 849 (1986) 193–202.
[49] I. Moya, M. Hodges, J.C. Barbet, Modification of room-temperature picosecond chlorophyll fluorescence kinetics in green algae by photosystemII trap closure, FEBS Lett. 198 (1986) 256–262.
[50] G.H. Schatz, H. Brock, A.R. Holzwarth, Picosecond kinetics of fluorescence and absorbency changes in photosystemII particles excited at low photon density, Proc. Natl. Acad. Sci. U. S. A. 84 (1987) 8414–8418.
[51] H.J.K. Keuper, K. Sauer, Effect of photosystemII reaction center closure on nanosecond fluorescence relaxation kinetics, Photosynth. Res. 20 (1989) 85–103.
[52] F. Terjung, Reabsorption of chlorophyll fluorescence and its effects on the spectral distribution and the picosecond decay of higher plant leaves, Z. Naturforsch. C J. Biosci. 53 (1998) 924–926.
[53] M. Mozzo, F. Passarini, R. Bassi, H. van Amerongen, R. Croce, Photoprotection in higher plants: The putative quenching site is conserved in all outer light-harvesting complexes of photosystem II, Biochim. Biophys. Acta Bioenerg. 1777 (2008) 1263–1267.
[54] A.V. Ruban, M.P. Johnson, C.D.P. Duffy, The photoprotective molecular switch in the photosystem II antenna, Biochim. Biophys. Acta Bioenerg. 1817 (2012) 167–181.
[55] A.R. Holzwarth, Y. Miloslavina, M. Nilkens, P. Jahns, Identification of two quenching sites active in the regulation of photosynthetic light-harvesting studied by time-resolved fluorescence, Chem. Phys. Lett. 483 (2009) 262–267.
[56] A.A. Pascal, et al., Molecular basis of photoprotection and control of photosynthetic light-harvesting, Nature 436 (2005) 134–137.
[57] H. Kirchhoff, S. Lenhert, C. Büchel, L. Chi, J. Nield, Probing the organization of photosystem II in photosynthetic membranes by atomic force microscopy, Biochemistry 47 (2008) 431–440.
[58] H. Kirchhoff, Molecular crowding and order in photosynthetic membranes, Trends Plant Sci. 13 (2008) 201–207.
[59] W. Wang, J. Chen, C. Li, W. Tian, Achieving solar overall water splitting with hybrid photosystems of photosystem II and artificial photocatalysts, Nat. Commun. 5 (4647) (2014), http://dx.doi.org/10.1038/ncomms5647.
[60] P.A. Albertsson, A quantitative model of the domain structure of the photosynthetic membrane, Trends Plant Sci. 6 (2001) 349–354.
[61] J. Breton, N.E. Geacintov, Picosecond fluorescence kinetics and fast energy-transfer processes in photosynthetic membranes, Biochim. Biophys. Acta 594 (1980) 1–32.
[62] V. Barzda, et al., Singlet-singlet annihilation kinetics in aggregates and trimers of LHCII, Biophys. J. 80 (2001) 2409–2421.
[63] D. Rutkauskas, J. Chmeliov, M. Johnson, A. Ruban, L. Valkunas, Exciton annihilation as a probe of the light-harvesting antenna transition into the photoprotective mode, Chem. Phys. 404 (2012) 123–128.